

Fig.6.1. Dark conductivity (\bullet , $a\text{-Si}_{1-x}\text{Ge}_x\text{:H}$; \blacksquare , $a\text{-Si:H}$; and \blacktriangle , $a\text{-Si}_{1-x}\text{C}_x\text{:H}$) and photoconductivity (\circ , $a\text{-Si}_{1-x}\text{Ge}_x\text{:H}$; \square , $a\text{-Si:H}$; and \triangle , $a\text{-Si}_{1-x}\text{C}_x\text{:H}$) under AM1 (100 mW/cm^2) of undoped films with various optical gaps.

CHAPTER VI CHANGES OF MIDGAP STATES

6-2. Midgap-state Profiles in Undoped Hydrogenated Amorphous Silicon-based Alloys

Undoped a-Si:H films and undoped a-Si_{1-x}C_x:H films were deposited using a diode-type rf glow-discharge reactor from pure SiH₄ gas and H₂/SiH₄/CH₄ gas mixture, respectively. Undoped a-Si_{1-x}Ge_x:H films with an optical gap (E_0) of 1.30 and 1.44 eV were deposited using a diode-type rf glow-discharge reactor from H₂/GeH₄/SiH₄ gas mixture, and undoped a-Si_{1-x}Ge_x:H ($1.55 \text{ eV} \leq E_0 \leq 1.70 \text{ eV}$) films were prepared using a triode-type rf glow-discharge reactor from GeH₄/SiH₄ gas mixture. The thicknesses were between 0.5 and 1.2 μm .

The heterojunctions were fabricated by depositing the amorphous films onto p-type crystalline silicon (p c-Si) substrates with an acceptor density (N_A) of $1.0 \times 10^{16} \text{ cm}^{-3}$, heated to 250 °C, and then evaporating Mg on an area (0.785 mm²) of those films at room temperature. Mg formed a good Ohmic contact with those amorphous films. All the heterojunctions exhibited good rectifying properties. The samples for measurements of optical gap, conductivity, photothermal deflection spectroscopy (PDS) and ESR were fabricated by depositing the amorphous films onto fused silica substrates heated to 250 °C.

The capacitance was measured using a Sanwa MI-415 capacitance meter (2 MHz). The transient HMC was measured as a function of temperature in the range between 213 and 413 K.

Figure 6.1 shows the dark conductivity and photoconductivity of films used in this study, indicating that the quality of the films was good. The Ge contents (x) determined from electron probe microanalysis (EPMA) in a-Si_{1-x}Ge_x:H were 0.80, 0.48, 0.44, and 0.27 for $E_0=1.30$, 1.55, 1.63, and 1.70 eV, respectively. The C contents (x) determined from Auger electron spectroscopy (AES) in a-Si_{1-x}C_x:H were 0.11 and 0.15 for $E_0=1.80$ and 1.88 eV, respectively. The Urbach energies obtained from PDS were 73, 58, 52, 62, 50, 84, and 87 meV for $E_0=1.30$, 1.55, 1.63, 1.70, 1.76, 1.80, and 1.88 eV, respectively. The Urbach energy is considered to be related with the slope in the valence-band tail.

Figure 6.2 shows the relation between the optical gap (E_0)

CHAPTER VI CHANGES OF MIDGAP STATES

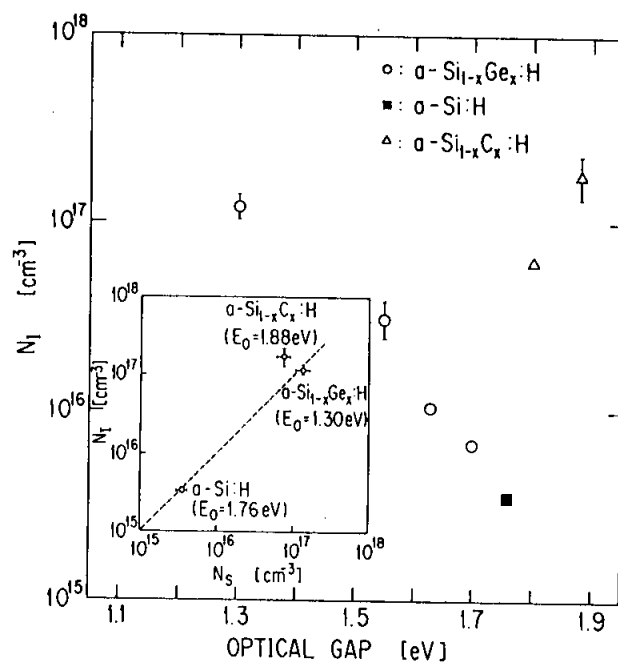


Fig.6.2. Densities (N_I) of midgap states of undoped films with various optical gaps. The relation between N_I and bulk spin density (N_S) obtained from ESR is inserted.

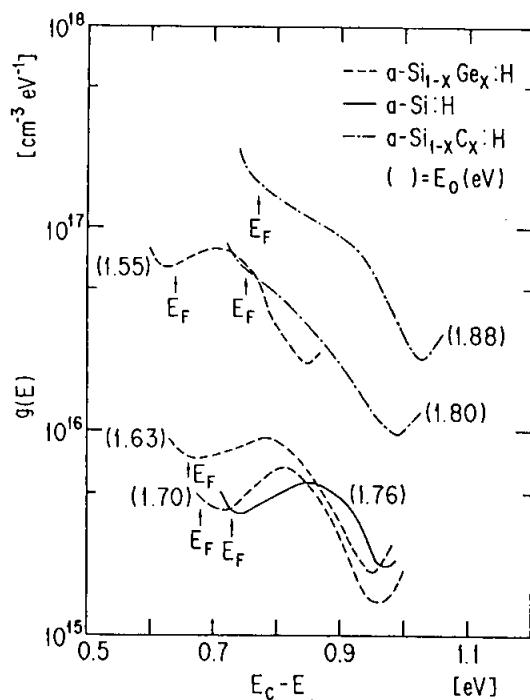


Fig.6.3. Density-of-state distributions in undoped films with various optical gaps.

CHAPTER VI CHANGES OF MIDGAP STATES

and the density of midgap states (N_I) obtained from the steady-state HMC method, and the relationship between N_I and the bulk spin densities (N_S) from ESR which represent the density of D^0 is inserted. The density of midgap states increases slowly with the Ge content, while it increases rapidly with the C content. This optical-gap dependence of the midgap-state density coincides with the result obtained from PDS, where the midgap-state density obtained from PDS is reported to be proportional to N_S . As is clear from the inserted figure, furthermore, the value of N_I is close to the corresponding bulk ESR spin density where surface state contributions were estimated by results from a series of films over a range of thicknesses, indicating N_I represents the density of D^0 in the bulk.

The g values obtained from ESR were 2.018, 2.006, and 2.005 for $a\text{-Si}_{1-x}\text{Ge}_x\text{:H}$ ($E_0=1.30$ eV), $a\text{-Si:H}$ ($E_0=1.76$ eV), and $a\text{-Si}_{1-x}\text{C}_x\text{:H}$ ($E_0=1.88$ eV), respectively. Shimizu et al.¹⁰⁾ have reported that the g values for dangling bonds of Ge, Si, and C are 2.019, 2.005, and 2.003, respectively. Morimoto et al.¹¹⁾ have reported that the ratio of Ge dangling bonds to Ge atoms is higher by a factor of four to fifteen than the ratio of Si dangling bonds to Si atoms in $a\text{-Si}_{1-x}\text{Ge}_x\text{:H}$ films. According to their experimental results, N_I in $a\text{-Si}_{1-x}\text{Ge}_x\text{:H}$ with $E_0 \leq 1.63$ eV represents the D^0 density of Ge. In $a\text{-Si}_{1-x}\text{C}_x\text{:H}$ ($E_0 \leq 1.88$ eV) and $a\text{-Si:H}$, N_I represents the D^0 density of Si. The value of N_I for the C content of 0.15 was $1.7 \times 10^{17} \text{ cm}^{-3}$ although N_I for the Ge content of 0.27 was $6.5 \times 10^{15} \text{ cm}^{-3}$, indicating that the ratio of Si dangling bonds to Si atoms in $a\text{-Si}_{1-x}\text{C}_x\text{:H}$ should be much higher than that in $a\text{-Si}_{1-x}\text{Ge}_x\text{:H}$. This indication seems reasonable in the light of bonding energies ($\text{Ge-H} < \text{Si-H} < \text{C-H}$), in other words, preferential attachment of H to Ge, Si, and C. Thus, incorporating a small amount of C into $a\text{-Si:H}$ causes C atoms to take H atoms from Si-H bonds near the surface of the film during the deposition, resulting in formation of excess Si dangling bonds.

Figure 6.3 shows six $g(E)$ corresponding to E_0 , which are estimated from the transient HMC method. Here, the attempt-to-escape frequencies (ν_n) for electrons which were experimentally

CHAPTER VI CHANGES OF MIDGAP STATES

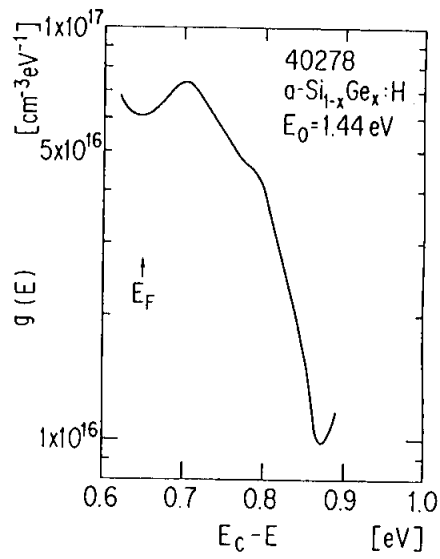


Fig.6.4. Density-of-state distribution for $\text{a-Si}_{1-x}\text{Ge}_x\text{:H}$ ($E_0=1.44 \text{ eV}$).

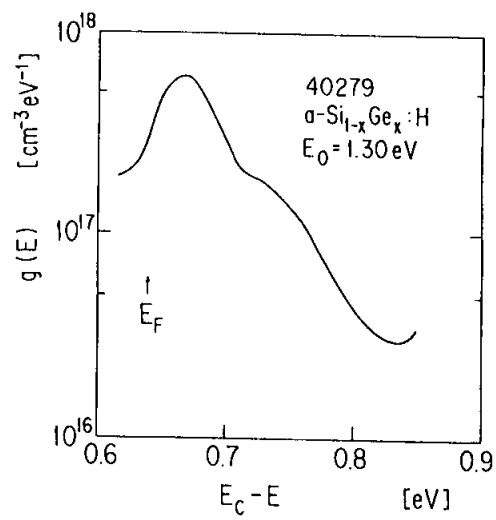


Fig.6.5. Density-of-state distribution for $\text{a-Si}_{1-x}\text{Ge}_x\text{:H}$ ($E_0=1.30 \text{ eV}$).

CHAPTER VI CHANGES OF MIDGAP STATES

obtained were 4×10^{12} , 1×10^{12} , 8×10^{11} , 4×10^{11} , 4×10^{11} , and 8×10^{11} s^{-1} for $E_0 = 1.55$, 1.63 , 1.70 , 1.76 , 1.80 , and 1.88 eV, respectively, and they were used to estimate the $g(E)$, as described in Chapter V. As the Ge content increases in the film, the energy location of the peak of $g(E)$ is shifted slowly toward the conduction band. In the figure, however, the two peaks of dangling bonds of Si and Ge cannot be seen. Figure 6.4 shows the $g(E)$ for $\text{a-Si}_{1-x}\text{Ge}_x\text{:H}$ ($E_0 = 1.44$ eV) with $\nu_n = 1 \times 10^{14} \text{ s}^{-1}$, which is obtained from Fig. 5.4. Figure 6.5 depicts the $g(E)$ for $\text{a-Si}_{1-x}\text{Ge}_x\text{:H}$ ($E_0 = 1.30$ eV) with $\nu_n = 3 \times 10^{14} \text{ s}^{-1}$. Both the films were deposited using an inductively-coupled rf glow-discharge reactor from $\text{H}_2/\text{GeH}_4/\text{SiH}_4$ gas mixture on p c-Si substrates heated to 200°C . As is clear from the study of ESR, both the main midgap states are D^0 of Ge. In the figures, therefore, both the main peaks of their $g(E)$ should arise from D^0 of Ge, and the shoulders, which appear in the right-hand side, must result from D^0 of Si.

In the case of $\text{a-Si}_{1-x}\text{C}_x\text{:H}$ ($E_0 \leq 1.88$ eV), as is clear from ESR, the main midgap states originate from D^0 of Si, indicating that the $g(E)$ shown in Fig. 6.3 should represent the distribution of singly-occupied Si dangling bonds. From the fact that the peak of $g(E)$ does not appear clearly in $\text{a-Si}_{1-x}\text{C}_x\text{:H}$, however, the singly-occupied Si dangling bonds are considered to be distributed in energy wider than them in a-Si:H . Since the ratio of Si dangling bonds to Si atoms in $\text{a-Si}_{1-x}\text{C}_x\text{:H}$ becomes higher than that in a-Si:H , the limitation on formation of Si dangling bonds in $\text{a-Si}_{1-x}\text{C}_x\text{:H}$ should get looser than that in a-Si:H , and the energy location of the Si dangling bonds in $\text{a-Si}_{1-x}\text{C}_x\text{:H}$ are allowed to broaden, coinciding with the broaden of their $g(E)$ shown in Fig. 6.3.

As indicated in Fig. 6.3, the energy location of D^0 in a-Si:H is around 0.85 eV below the conduction band edge, which belongs to group B classified by LeComber and Spear,¹⁾ whereas group A has insisted that the energy location of D^0 of Si is around 1.1 eV. These results for the peak energy location of D^0 in $\text{a-Si}_{1-x}\text{Ge}_x\text{:H}$ coincides with the results obtained by Tsutsumi et al.¹²⁾ who could not, however, determine the $g(E)$ of D^0 .

CHAPTER VI CHANGES OF MIDGAP STATES

Since there are only a few data concerned with the peak energy location of D^0 in $a\text{-Si}_{1-x}\text{Ge}_x\text{:H}$ and there is no data concerned with that in $a\text{-Si}_{1-x}\text{C}_x\text{:H}$, a lot of researches determining their energy location should be performed by means of different techniques.

6-3. Thermal Recovery Process of Midgap-state Profile of Light-soaked Undoped $a\text{-Si:H}$

Undoped $a\text{-Si:H}$ films (about $1.2\ \mu\text{m}$ thickness) were deposited by the rf glow-discharge decomposition of pure SiH_4 . In order to measure dark conductivity (σ_2), photoconductivity ($\Delta\sigma_{ph}$), and the activation energy ($\delta_2 = E_C - E_F$) of dark conductivity in $a\text{-Si:H}$ films, samples with coplanar electrodes were fabricated by depositing $a\text{-Si:H}$ onto Corning 7059 glass substrates heated to $250\ ^\circ\text{C}$ for sample 21099 and heated to $310\ ^\circ\text{C}$ for sample AK362, and subsequently by evaporating Al at room temperature. Thus-determined properties are shown in Table 6-1. Oxygen, carbon, and nitrogen concentrations estimated using secondary-ion mass spectrometry (SIMS) were 7×10^{19} , 1×10^{19} , and $3 \times 10^{18}\ \text{cm}^{-3}$ in sample 21099, respectively, and they were 5×10^{19} , 2×10^{19} , and $8 \times 10^{17}\ \text{cm}^{-3}$ in sample AK362, respectively.

The heterojunctions were fabricated by depositing the films onto p c-Si substrates heated to $250\ ^\circ\text{C}$ for sample 21099 and heated to $310\ ^\circ\text{C}$ for sample AK362. The acceptor density (N_A) of p c-Si was $1.0 \times 10^{16}\ \text{cm}^{-3}$. Since Mg has been known to form a good Ohmic contact with undoped $a\text{-Si:H}$, Mg was then evaporated on an area ($0.785\ \text{mm}^2$) of as-deposited $a\text{-Si:H}$ films at room temperature. For other heterojunctions, Mg was evaporated after $a\text{-Si:H}$ films were exposed to the AM1 light with $100\ \text{mW/cm}^2$ at room temperature. As soon as the sample 21099 heated to $150\ ^\circ\text{C}$ in a vacuum, the transient HMC was measured using the Sanwa MI-415 capacitance meter (2 MHz). It was also measured 30-min later, 1-h later, and 2-h later. However, the transient HMC of sample AK362 could not be measured at $150\ ^\circ\text{C}$ because of low resistivity of its $a\text{-Si:H}$ film. Therefore, after the sample was